Activation of the endoplasmic reticulum unfolded protein response by lipid disequilibrium without disturbed proteostasis in vivo

Nicole S. Hou[a,b,c], Aljona Gutschmidt[d,e], Daniel Y. Choi[a,b], Keouna Pather[a,b], Xun Shi[f], Jennifer L. Watts[f], Thorsten Hoppe[d,e], and Stefan Taubert[a,b,c,g,1]

[a]Centre for Molecular Medicine and Therapeutics and [b]Child and Family Research Institute, Vancouver, BC, Canada V5Z 4H4; [c]Graduate Program in Cell and Developmental Biology and [g]Department of Medical Genetics, University of British Columbia, Vancouver, BC, Canada V5Z 4H4; [d]Institute for Genetics and [e]Cologne Excellence Cluster on Cellular Stress Responses in Aging-Associated Diseases, University of Cologne, 50931 Cologne, Germany; and [f]School of Molecular Biosciences, Washington State University, Pullman, WA 99164

Edited by Gary Ruvkun, Massachusetts General Hospital, Boston, MA, and approved April 24, 2014 (received for review September 27, 2013)

The Mediator is a conserved transcriptional coregulator complex required for eukaryotic gene expression. In *Caenorhabditis elegans*, the Mediator subunit *mdt-15* is essential for the expression of genes involved in fatty acid metabolism and ingestion-associated stress responses. *mdt-15* loss of function causes defects in reproduction and mobility and shortens lifespan. In the present study, we find that worms with mutated or depleted *mdt-15* (*mdt-15* worms) exhibit decreased membrane phospholipid desaturation, especially in phosphatidylcholine. Accordingly, *mdt-15* worms exhibit disturbed endoplasmic reticulum (ER) homeostasis, as indicated by a constitutively activated ER unfolded protein response (UPR^{ER}). Activation of this stress response is only partially the consequence of reduced membrane lipid desaturation, implicating other *mdt-15*–regulated processes in maintaining ER homeostasis. Interestingly, *mdt-15* inactivation or depletion of the lipid metabolism enzymes stearoyl-CoA-desaturases (*SCD*) and S-adenosyl methionine synthetase (*sams-1*) activates the UPR^{ER} without promoting misfolded protein aggregates. Moreover, these worms exhibit wild-type sensitivity to chemically induced protein misfolding, and they do not display synthetic lethality with mutations in UPR^{ER} genes, which cause protein misfolding. Therefore, the constitutively activated UPR^{ER} in *mdt-15*, *SCD*, and *sams-1* worms is not the consequence of proteotoxic stress but likely is the direct result of changes in ER membrane fluidity and composition. Together, our data suggest that the UPR^{ER} is induced directly upon membrane disequilibrium and thus monitors altered ER homeostasis.

mediator complex | MED15 | cardiolipin | *C. elegans*

Transcriptional regulation is crucial for organism survival and development. In eukaryotes, the expression of most protein-coding genes requires a conserved transcriptional coregulator complex called the "Mediator" (1, 2). The Mediator is composed of 25–30 subunits, depending on species. Although some Mediator subunits are universally required for gene expression, others affect only subsets of genes (1, 2). In the nematode *Caenorhabditis elegans*, the Mediator subunit MDT-15 specifically regulates the transcription of genes involved in fatty acid (FA) metabolism and ingestion-associated stress responses (3–5). *mdt-15* depletion by feeding RNA interference (RNAi) (6) or *mdt-15* reduction-of-function mutation (7) results in phenotypes such as developmental arrest, sterility, defective locomotion, a shortened lifespan, and stress sensitivity (3–5). These phenotypes occur in part because *mdt-15* is required to express three genes encoding FA Δ9-desaturases [*fat-5*, *fat-6*, and *fat-7*, the latter two collectively referred to as "stearoyl-CoA-desaturases" (SCDs) (8, 9)]. Dietary supplementation with the downstream products of these desaturases partially rescues the phenotypes of *mdt-15(RNAi)* worms (3, 4). However, why *mdt-15*–mediated processes such as FA synthesis are so broadly and fundamentally required for organism survival and development remains unclear.

FAs are important components of most lipids. Both the length and the degree of saturation of the fatty acyl chains determine the chemical properties of lipids and thus the biological functions of lipid membranes (10, 11). Alterations in membrane lipid desaturation and aberrant phospholipid (PL) composition can severely disrupt homeostasis of the endoplasmic reticulum (ER), a membrane-bound organelle (12–14). The ER is the major subcellular compartment for protein and lipid biosynthesis and for calcium storage (14, 15). Because of these fundamental roles, metazoans have evolved a conserved signaling circuit called the "ER unfolded protein response" (UPR^{ER}) to protect against ER stress. ER stress is considered the consequence of the accumulation of misfolded proteins in the ER, and misfolded proteins trigger UPR^{ER} activation through three parallel pathways: the inositol-requiring-enzyme 1 (IRE-1) branch, the protein kinase RNA-like ER kinase (PERK) branch, and the activating transcription factor 6 (ATF-6) branch (16). Signaling through these pathways induces the expression of chaperones, lipid synthesis enzymes, and oxidative stress-response factors as well as general translational attenuation and, upon prolonged UPR^{ER} activation, apoptosis (14–16). Together, this transcriptional and translational reprogramming mitigates ER stress and improves ER protein-handling capacity. The association of disrupted ER homoeostasis with diseases such as neurodegenerative disorders and obesity-

Significance

The unfolded protein response of the endoplasmic reticulum (UPR^{ER}) is induced by proteotoxic conditions. Lipid disequilibrium also activates the UPR^{ER}, but whether this activation is accompanied by disturbed proteostasis in vivo remains controversial. In this study, we show that in the nematode *Caenorhabditis elegans* compromised fatty acid desaturation and reduced phosphatidylcholine production activate the UPR^{ER} without overt proteostatic imbalance, as assessed by molecular, pharmacological, and genetic analyses. This finding suggests that membrane composition is a direct input able to activate UPR^{ER} signaling even when proteostasis in the ER is largely intact. The activation of the UPR^{ER} by independent inputs may reflect the central role of the ER in both lipid and protein biosynthesis.

Author contributions: N.S.H. and S.T. designed research; N.S.H., A.G., D.Y.C., K.P., X.S., J.L.W., and S.T. performed research; N.S.H., A.G., and T.H. contributed new reagents/analytic tools; N.S.H., A.G., J.L.W., and S.T. analyzed data; and N.S.H., A.G., J.L.W., T.H., and S.T. wrote the paper.

The authors declare no conflict of interest.

This article is a PNAS Direct Submission.

Freely available online through the PNAS open access option.

[1]To whom correspondence should be addressed. E-mail: taubert@cmmt.ubc.ca.

This article contains supporting information online at www.pnas.org/lookup/suppl/doi:10.1073/pnas.1318262111/-/DCSupplemental.

induced insulin resistance highlights the importance of ER homeostasis (15, 17).

Unfolded proteins directly bind the ER-luminal sensor domain of yeast Ire1p (18), but the precise molecular mechanisms that activate each UPR^{ER} sensor remain incompletely understood. Interestingly, in yeast, in cultured mammalian cells, and in mice, ER membrane disequilibrium also activates the UPR^{ER}; because chemical chaperones, which improve protein-folding capacity in the ER, alleviate UPR^{ER} induction in these contexts, it is likely that these lipid alterations indirectly affect ER proteostasis (19, 20). However, recent evidence suggests that IRE1 and PERK retain the ability to activate the UPR^{ER} even without a functional unfolded protein sensing domain (21, 22), indicating that membrane lipid perturbations directly activate the UPR^{ER}.

In this study, we set out to dissect *mdt-15*'s role in FA homeostasis. We show that *mdt-15* is crucial for membrane lipid synthesis by maintaining membrane PL desaturation, especially in the dominant ER membrane lipid phosphatidylcholine (PC). *mdt-15*–regulated FA desaturation is critical for ER homeostasis, because *mdt-15* inactivation induces a constitutively activated UPR^{ER} that is partially suppressed by unsaturated FA supplementation. In contrast, *mdt-15* inactivation does not induce the mitochondrial unfolded protein response (UPR^{mito}), a pathway that is molecularly distinct from the UPR^{ER} (23). Intriguingly, the *mdt-15*–induced UPR^{ER} occurs without causing misfolded-protein aggregation in the ER and without hypersensitizing animals to chemically or genetically induced proteotoxic stress. Furthermore, inactivating PL synthesis enzymes also activates the UPR^{ER} without causing proteotoxic stress. Thus, the *mdt-15*–regulated lipid balance is linked to a distinct type of ER stress that is independent of proteostasis. Our data suggest that the UPR^{ER} represents a general ER surveillance pathway capable of assessing not only protein homeostasis but also mem brane integrity.

Results

mdt-15 Is Required to Maintain Normal Membrane Lipid Composition. The chemical and biophysical properties of membrane lipids depend on their fatty acyl compositions (10, 11). Depleting *mdt-15* by RNAi causes an overall shift from unsaturated to saturated FAs (3, 4), but the physiological relevance and effects on membrane PLs and triglyceride (TG) have not yet been studied. To obtain comprehensive insight into the role of *mdt-15* in lipid fatty acyl compositions, we extracted total lipids from *mdt-15(RNAi)* worms and hypomorph *mdt-15(tm2182)* mutants, separated them by thin-layer chromatography (TLC), and quantified the FA compositions of individual lipids using gas chromatography–mass spectrometry (GC-MS). Consistent with previous findings (3, 4), we observed an overall increase in saturated FAs and an overall decrease in polyunsaturated FAs (PUFAs) in *mdt-15* worms (Fig. 1*A* and Fig. S1 *A*–*C*). The up-regulation in lipid saturation and the down-regulation in lipid polyunsaturation arose from both membrane PLs and TG (Fig. 1*B* and Fig. S1*C*). Interestingly, although both PC and phosphatidylethanolamine (PE) are major membrane PLs, PC desaturation was affected more substantially by *mdt-15* inactivation (Fig. 1 *B*–*D* and Fig. S1 *A*–*E*; see Tables S1–S6 for *P* values). This difference also was evident in the abundance of respective FA species in individual PLs. For instance, the PUFA C20:5 was much more strongly reduced in PC than in PE (Fig. 1 *C* and *D* and Fig. S1 *D* and *E*). In contrast to the FA compositions, the overall relative levels of membrane PLs and TG were relatively similar in *mdt-15* and control worms: We observed only a slight decrease of PC in *mdt-15(RNAi)* worms (Fig. 1*E*) and no significant decrease in *mdt-15(tm2182)* mutants (Fig. S1*F*). The slight change in *mdt-15(RNAi)* worms most likely reflects the severe down-regulation of PUFAs (see below, Fig. 2*F* and Fig. S2*F*). Taken together, our data suggest that *mdt-15* is required for maintaining normal FA unsatura-

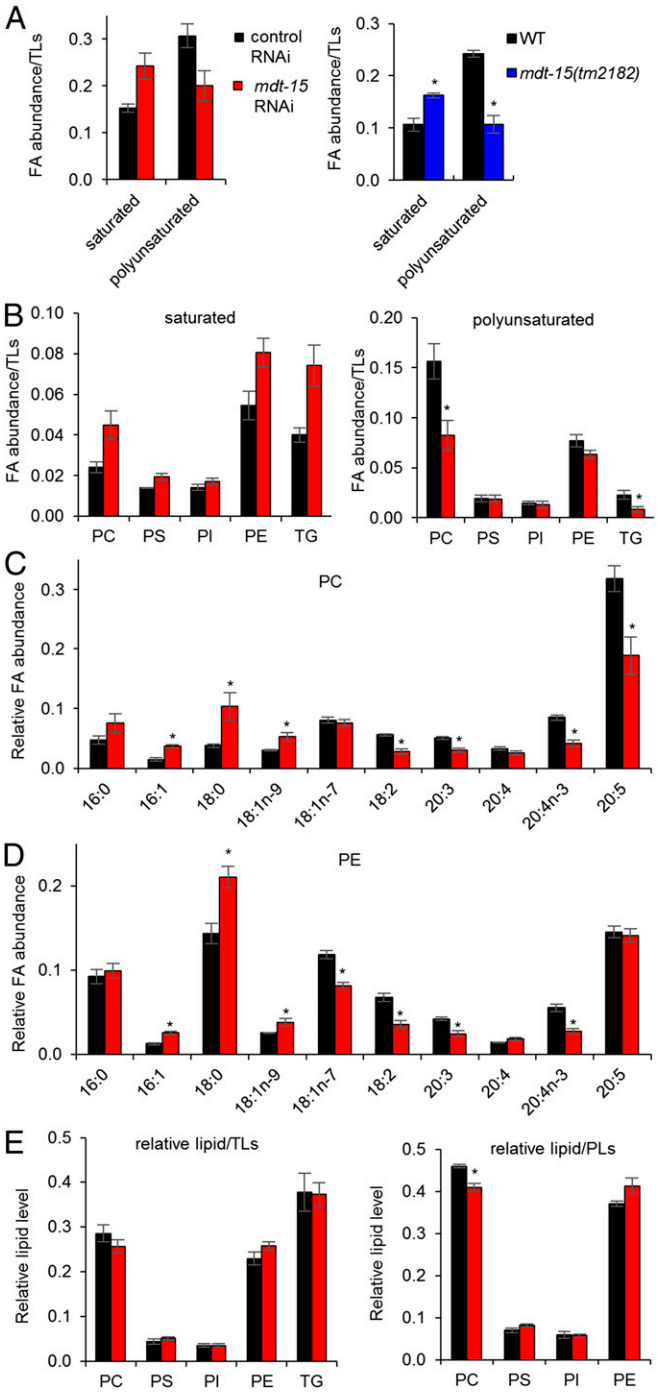

Fig. 1. *mdt-15* is required for maintaining membrane lipid desaturation. (*A*) Bars represent the average abundance of saturated and polyunsaturated lipids, including PLs and TG, relative to total lipids (TLs). Saturated lipids are the fraction of the above lipids containing C16:0 and/or C18:0 fatty acyl chains; polyunsaturated lipids are lipids with C18:2, C20:3, C20:4, C20:4n-3, and/or C20:5 fatty acyl chains. (*B*) Bars indicate the average abundance of saturated and polyunsaturated fatty acyl chains in PC, phosphatidylserine (PS), phosphatidylinositol (PI), PE, and TG, relative to total lipids. (*C*) Bars represent the relative abundance of individual FAs in PC. (*D*) Bars represent the relative abundance of individual FAs in PE. (*E*) Bars indicate the average levels of individual lipid species relative to TLs (*Left*) and relative to total PLs (*Right*). In all panels, lipids were isolated from L4-stage *control(RNAi)*, *mdt-15(RNAi)*, wild-type (WT), or *mdt-15 (tm2182)* worms ($n = 3$). Error bars represent SEM; $^*P < 0.05$ (two-tailed Student *t* test). For *P* values, see Tables S1–S6.

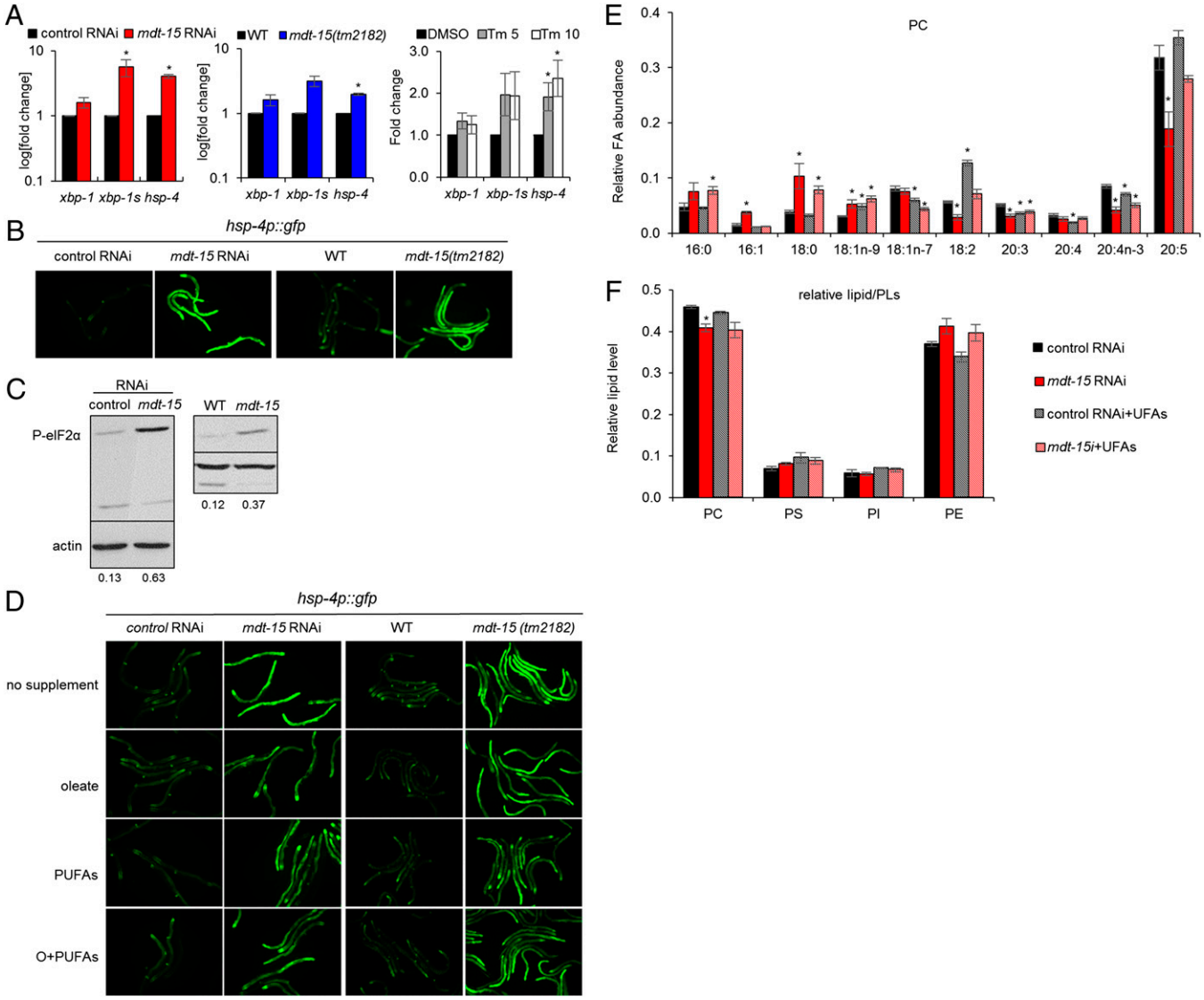

Fig. 2. *mdt-15* inactivation alters membrane lipid composition and induces the UPR^{ER}. (*A*) Bar graphs represent the average fold change of *xbp-1*, spliced *xpb-1* (*xbp-1s*), and *hsp-4* mRNA levels in *control(RNAi)* and *mdt-15(RNAi)* worms ($P = 0.098$, 0.049, and 0.00049, respectively) (*Left*), WT and *mdt-15(tm2182)* worms ($P = 0.19$, 0.063, and 0.0064, respectively) (*Center*), or *control(RNAi)* worms treated with DMSO, 5 μg/mL tunicamycin (Tm 5; $P = 0.16$, 0.13, 0.04, respectively) or 10 μg/mL tunicamycin (Tm 10; $P = 0.31$, 0.18, 0.03, respectively) (*Right*). $n = 3$ for all experiments; error bars represent SEM; $^*P < 0.05$ (two-tailed Student *t* test). (*B*) Micrographs depict *control(RNAi)* and *mdt-15(RNAi)* worms or WT and *mdt-15(tm2182)* worms expressing the *hsp-4p::GFP* transcriptional reporter; one of four independent experiments is shown. (*C*) Immunoblots depict the levels of phospho-Ser51 eIF2α (P-eIF2α) and actin protein levels in *control(RNAi)*, *mdt-15(RNAi)*, WT, and *mdt-15(tm2182)* worms. The numbers represent the intensity of the P-eIF2α bands relative to corresponding actin bands. One of four independent experiments is shown. (*D*) Micrographs show *control(RNAi)* and *mdt-15(RNAi)* worms or WT and *mdt-15(tm2182)* worms expressing the *hsp-4p::GFP* transcriptional reporter grown without dietary supplements (no supplement), with 300 μM C18:1n-9 (oleate), with 150 μM C18:2 and 150 μM C20:5 (PUFAs), or with 150 μM C18:1n-9 and 300 μM PUFAs (O+PUFAs). (*E*) Bars represent the relative abundance of individual FAs in PC. (*F*) Bars represent the average levels of individual lipid species relative to total PLs. For *E* and *F*, lipids were extracted from L4-stage *control(RNAi)* or *mdt-15(RNAi)* worms raised in the absence or presence of dietary unsaturated FAs (UFAs; C18:1n-9, C18:2, and C20:5). $n = 3$; error bars represent SEM; $^*P < 0.05$ as determined by two-tailed Student *t* test. For *P* values, see Tables S1–S3.

tion but does not strongly influence the relative levels of PLs and TGs.

***mdt-15*–Mediated Lipid Desaturation Is Essential for ER Homeostasis.** The degree of saturation and the chain length of fatty acyl tails strongly influence membrane PL structure and thus the function of cellular organelles (10, 11, 14). For instance, the ER requires a more fluidic membrane to accommodate protein and/or lipid biosynthesis. Because the ER membrane is enriched in PC, which is most profoundly altered by *mdt-15* depletion or mutation, we hypothesized that *mdt-15* is required for ER homeostasis. To test this hypothesis, we determined whether the UPR^{ER} is induced in worms lacking *mdt-15*. In metazoans, activation of the IRE-1 branch of the UPR^{ER} results in increased splicing of the mRNA encoding the transcription factor X-box–binding protein 1 (XBP-1), which activates UPR^{ER} target genes such as the ER-specific chaperone and heat-shock protein *hsp-4*/*BiP* (16). Using *hsp-4* and spliced *xbp-1* (*xbp-1s*) as markers, we found that loss of *mdt-15* resulted in chronic UPR^{ER} activation, as indicated by an increase in *xpb-1s* and *hsp-4* mRNA levels (Fig. 2*A*). This transcriptional response is similar to that of *control(RNAi)* worms treated with the protein glycosylation inhibitor and UPR^{ER} inducer tunicamycin

(24) (Fig. 2*A*), as reported previously (25). A transcriptional *hsp-4* reporter, *hsp-4p::GFP* (26), also was strongly up-regulated in *mdt-15(RNAi)* and *mdt-15(tm2182)* worms (Fig. 2*B*). The elevated expression of *hsp-4p::GFP* was abrogated by concurrent loss of *xbp-1* (Fig. S2*A*), demonstrating that *hsp-4* induction in *mdt-15* worms reflects canonical UPR^{ER} signaling (26). Furthermore, activation of the UPR^{ER} PERK arm attenuates general protein translation by phosphorylating and inhibiting the eukaryotic translation initiation factor eIF2α (16), and down-regulation of *mdt-15* substantially increased the levels of phosphorylated eIF2α (Fig. 2*C*). Thus, loss of *mdt-15* perturbs ER homeostasis and activates at least two branches of the canonical UPR^{ER}.

Decreased membrane lipid unsaturation induces the UPR^{ER} in mammalian cells and in yeast (12, 19, 27). Because *mdt-15* is required to maintain normal membrane PL unsaturation (Fig. 1 and Fig. S1), we hypothesized that *mdt-15* confers ER homeostasis by maintaining unsaturated FA levels. To test this hypothesis, we supplemented *mdt-15(RNAi)* and *mdt-15(tm2182)* worms with the FAs most strongly down-regulated following *mdt-15* depletion (C18:1n-9, C18:2, and C20:5). Using the *hsp-4p::GFP* reporter as an indicator for UPR^{ER} activation, we found that in *mdt-15(RNAi)* and *mdt-15(tm2182)* worms, oleic acid (C18:1n-9) alone and combinations of unsaturated FAs substantially but only partially suppressed *hsp-4p::GFP* induction and morphological phenotypes (Fig. 2*D* and Fig. S2*B*). Similarly, unsaturated FA supplementation significantly rescued the induced *hsp-4* and *xbp-1s* mRNA levels in *mdt-15(RNAi)* worms (Fig. S2*C*; note that the same FA supplements fully rescue the UPR^{ER} induction in the Δ9-desaturase-depleted *SCD(RNAi)* worms; also see Fig. 6*D*).

In principle, the failure of the dietary FAs to suppress completely the UPR^{ER} induction (and other phenotypes) in *mdt-15* worms could be due to defects in FA uptake or incorporation into organismal lipids. To test this possibility, we profiled lipids in *control(RNAi)*, *mdt-15(RNAi)*, and *SCD(RNAi)* worms grown in the presence of dietary unsaturated FAs (C18:1n-9, C18:2, and C20:5). Uptake and incorporation of the supplemented FAs was effective in both *control(RNAi)* and *mdt-15(RNAi)* worms: Both genotypes displayed a substantial increase in the fraction of the supplemented FAs in PC, and supplemented *mdt-15(RNAi)* worms resembled unsupplemented *control(RNAi)* worms (Fig. 2*E*). Moreover, the small reduction observed in the PC level of *mdt-15(RNAi)* worms also was suppressed by FA supplementation (Fig. 2*F*), indicating that defects in PUFA biosynthesis affect overall PC production [as is also the case in *SCD(RNAi)* worms; Fig. S2*F*]. In contrast to the PUFA levels in PC, which were normalized in supplemented *mdt-15(RNAi)* or *SCD(RNAi)* animals, the elevated content of saturated FAs such as C16:0 and C18:0 was not fully suppressed (Fig. 2*E* and Fig. S2 *D* and *E*). Together, these data suggest that the disrupted ER homeostasis in *mdt-15* worms is the consequence of reduced membrane PL polyunsaturation. Nevertheless, *mdt-15* also affects other processes that contribute to ER homeostasis.

***mdt-15* Is Not Part of the UPR^{ER}.** The UPR^{ER} is required for normal development and for survival under exogenous ER proteotoxic stress (26, 28). The inability to activate UPR^{ER} genes compromises the ER's protein-folding capacity and hypersensitizes cells and organisms to ER stress (29, 30). Thus, the activation of UPR^{ER} markers in *mdt-15* worms could arise from defects in the downstream activation of UPR^{ER} signaling. To test this hypothesis, we compared the genes induced by exogenous ER stress [inducible UPR^{ER} genes (29)] with those down-regulated or up-regulated in *mdt-15(RNAi)* worms (5). We found that the genes down-regulated in *mdt-15(RNAi)* worms did not overlap at all with inducible UPR^{ER} genes. In contrast, genes up-regulated by *mdt-15* depletion overlapped significantly with the inducible UPR^{ER} genes (Fig. 3*A*), in agreement with the notion that loss of *mdt-15* activates the UPR^{ER}. To test more directly whether *mdt-15* is required to induce UPR^{ER} genes, we quantified the transcript levels of three UPR^{ER} genes in *control(RNAi)* and *mdt-15(RNAi)* worms in the absence and presence of tunicamycin. We found that the induction of UPR genes by tunicamycin was not impaired in *mdt-15(RNAi)* worms. Conversely, these genes were constitutively up-regulated upon *mdt-15* depletion (Fig. 3*B*). Thus, *mdt-15* is not directly involved in the activation of the UPR^{ER}, but its depletion induces ER stress.

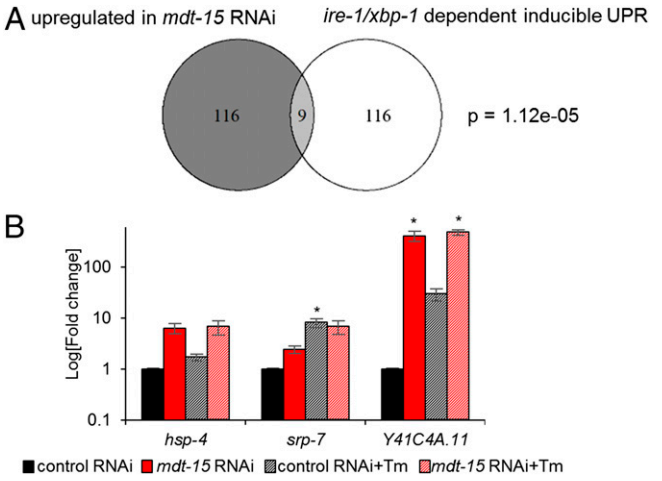

Fig. 3. *mdt-15* is not directly involved in the UPR^{ER}. (*A*) The Venn diagram shows the overlap between genes up-regulated in *mdt-15(RNAi)* worms and the *ire-1/xbp-1*–dependent inducible UPR genes. The *P* value was calculated using Fisher's exact test, as described (7). (*B*) Bar graphs represent the average fold change of mRNA levels in *control(RNAi)* and *mdt-15(RNAi)* worms treated with DMSO or 10 μg/mL tunicamycin; fold change is relative to DMSO-treated *control(RNAi)* worms. For *hsp-4*: $P = 0.069$, 0.12, and 0.11, respectively; for *srp-7*: $P = 0.069$, 0.05, and 0.10, respectively; and for Y41C4A.11: $P = 0.056$, 0.072, and 0.012, respectively. $n = 3$; error bars represent SEM; $^*P < 0.05$ as determined by two-tailed Student *t* test.

***mdt-15* Is Not Required for Mitochondrial Protein Homeostasis.** Like the ER, mitochondria are lipid-bound organelles that synthesize and modify proteins. Thus, we asked whether *mdt-15* is required only for ER homeostasis or also affects mitochondrial homeostasis. To address this question, we examined the expression of the mitochondrial chaperones *hsp-6* and *hsp-60*, which are specific to the UPR^{mito} (23). We found that *mdt-15* RNAi failed to induce the UPR^{mito} as determined with strains expressing transcriptional *hsp-6p::GFP* and *hsp-60p::GFP* reporters (Fig. 4*A*). To test whether *mdt-15* inactivation impairs the UPR^{mito}, we exposed worms to the electron transport chain inhibitor antimycin A, which activates the UPR^{mito}. We found that *mdt-15* depletion did not affect the induction of *hsp-6p::GFP* by antimycin A (Fig. 4*B*). Therefore, *mdt-15* does not influence mitochondrial homeostasis or the UPR^{mito}.

The UPR^{mito} is not affected in *mdt-15(RNAi)* worms despite the alterations in membrane lipid desaturation. Thus, we studied the composition and levels of cardiolipin, a PL class unique to mitochondria (31). Cardiolipin is found mainly in the inner mitochondrial membrane and in contact sites between the outer and inner mitochondrial membranes (31). We found that neither the FA composition nor the relative level of cardiolipin was affected by *mdt-15* depletion (Fig. 4*C*). Interestingly, the FA profiles of cardiolipin are quite distinct from those seen in other PLs of *C. elegans* and from those of cardiolipin in other metazoans (*Discussion*).

***mdt-15* Inactivation Induces the UPR^{ER} Without Disturbing ER Proteostasis.** UPR^{ER} activation is considered the consequence of unfolded protein accumulation in the ER. However, increased membrane lipid saturation triggers the UPR^{ER} in cultured cells that express

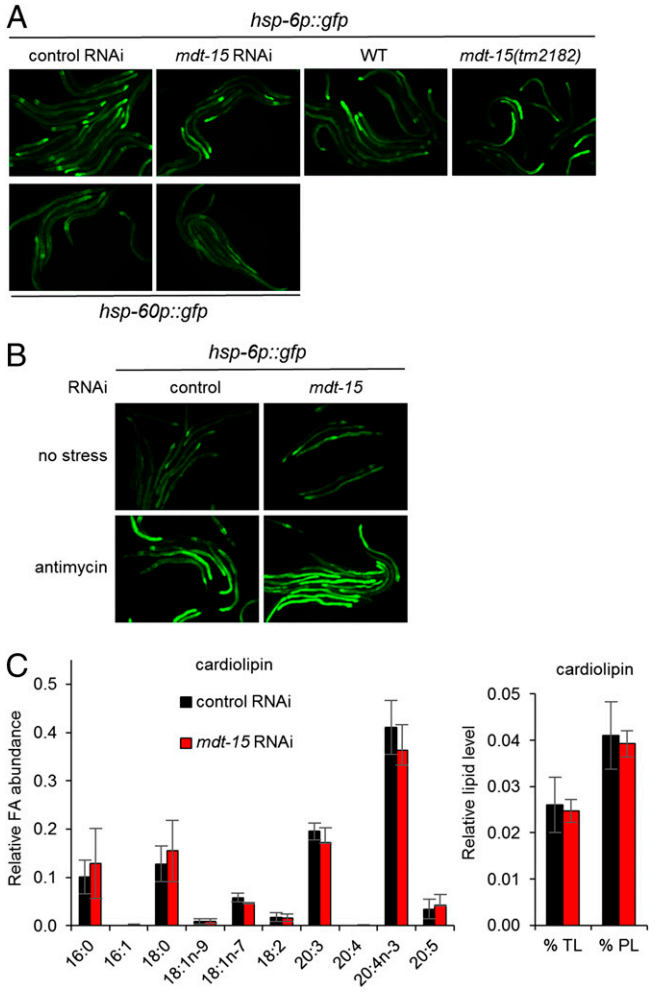

Fig. 4. *mdt-15* is not required for mitochondrial protein homeostasis. (*A*) Micrographs show *control(RNAi)*, *mdt-15(RNAi)*, WT, and *mdt-15(tm2182)* worms expressing the *hsp-6p::GFP* transcriptional reporter (*Upper row*) or the *hsp-60p::GFP* transcriptional reporter (*Lower row*). (*B*) Micrographs show *control(RNAi)* and *mdt-15(RNAi)* worms expressing the *hsp-6p::GFP* transcriptional reporter treated with 10 μg/mL antimycin A for 24 h (*Lower row*) or not treated (*Upper row*). For *A* and *B*, one of three independent experiments is shown. (*C*) Bars represent the relative abundance of individual FAs in cardiolipin (*Left*) and the average levels of cardiolipin relative to TLs or total PLs (*Right*). Lipids were extracted from *control(RNAi)* and *mdt-15(RNAi)* worms. $n = 3$; error bars represent SEM; $^*P < 0.05$ as determined by two-tailed Student *t* test.

IRE-1 and PERK mutants unable to sense misfolded proteins (21). Therefore, we hypothesized that loss of *mdt-15* does not impair protein folding. To test this hypothesis, we used a strain carrying a *vha-6p::SRP-2^{H302R}::GFP* transgene. SRP-2 is a *C. elegans* homolog of neuroserpin, and the H302R substitution causes ER-luminal SRP-2 aggregation, which is strongly enhanced in worms deficient for the UPR^{ER} or for the heat-shock factor HSF-1 (32). As shown previously (32), defects in the canonical UPR^{ER} pathways substantially enhance the aggregation of misfolded SRP-2^{H302R} (Fig. 5*A* and Fig. S3*A*). Depleting the ER-specific chaperone ENPL-1/GRP94 or the sarco-endoplasmic reticulum Ca^{2+} ATPase SCA-1, known regulators of ER proteostasis, also caused significant SRP-2^{H302R} aggregation (Fig. 5*A* and Fig. S3*A*) and, as reported (33, 34), induced the UPR^{ER} (Fig. 6*C* and Fig. S3*B*). In contrast, *mdt-15* depletion did not increase SRP-2^{H302R}::GFP aggregation (Fig. 5*A* and Fig. S3*A*). We observed similar results with another misfolded protein reporter, CPL-1^{W32A,Y35A}::YFP, a mutant of *C. elegans* procathepsin L that serves as a substrate for the ER-associated protein degradation (ERAD) machinery (35). *mdt-15* depletion did not cause an increase in CPL-1^{W32A,Y35A} levels, as determined by immunoblot (Fig. 5*B*; UPR^{ER} activation is shown in Fig. S3*B*). In contrast, depletion of UPR^{ER} genes or the essential ERAD component *sel-1*

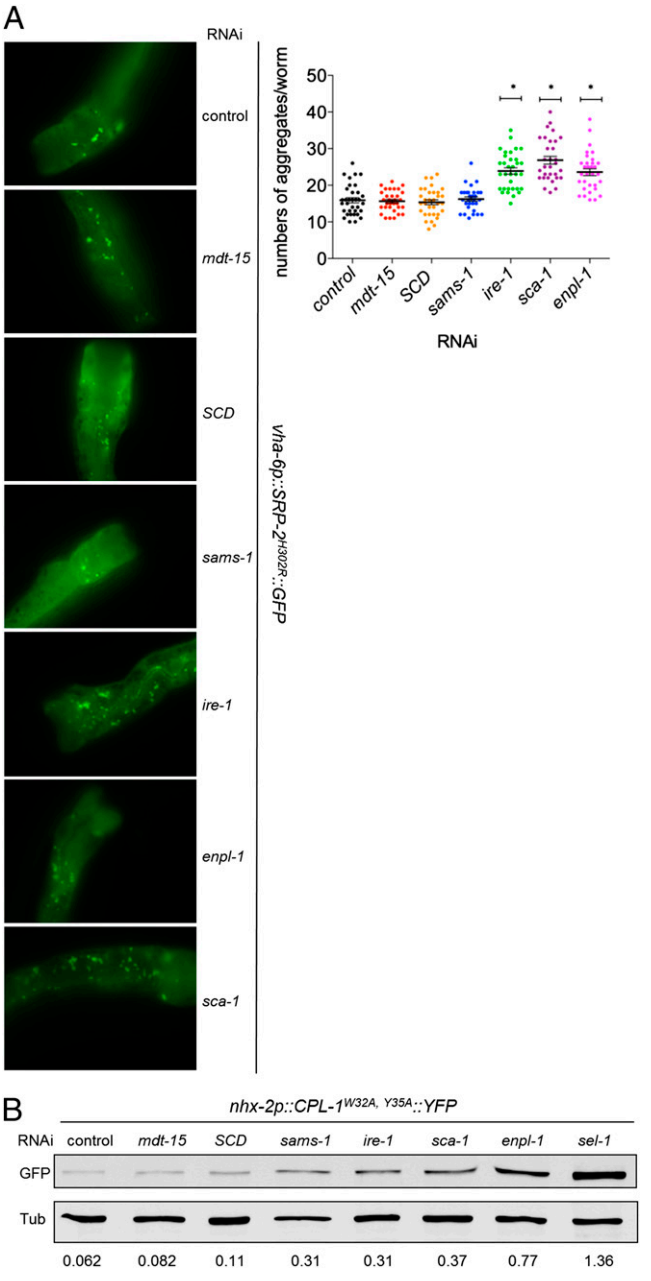

Fig. 5. *mdt-15* inactivation and defects in PL biosynthesis do not enhance misfolded-protein aggregation. (*A*, *Left*) Micrographs depict SRP-2^{H302R}::GFP foci in control, *mdt-15–*, *SCD-*, *sams-1–*, *ire-1–*, *enpl-1–*, and *sca-1*–depleted worms. (*Right*) The dot plot represents the quantification of GFP aggregates; data points were pooled from three independent experiments. $^*P < 0.0001$ compared with control RNAi. The nonsignificant *P* values are *mdt-15*, 0.89; *SCD*, 0.80; and *sams-1*, 0.48. (*B*) The immunoblot shows the levels of CPL-1^{W32A,Y35A}::YFP and tubulin (loading control) in lysates from control, *mdt-15–*, *SCD-*, *sams-1–*, *ire-1–*, *sca-1–*, *enpl-1–*, and *sel-1*–depleted worms. The numbers below the blots represent the intensity of the bands relative to corresponding tubulin bands. One of four independent experiments is shown.

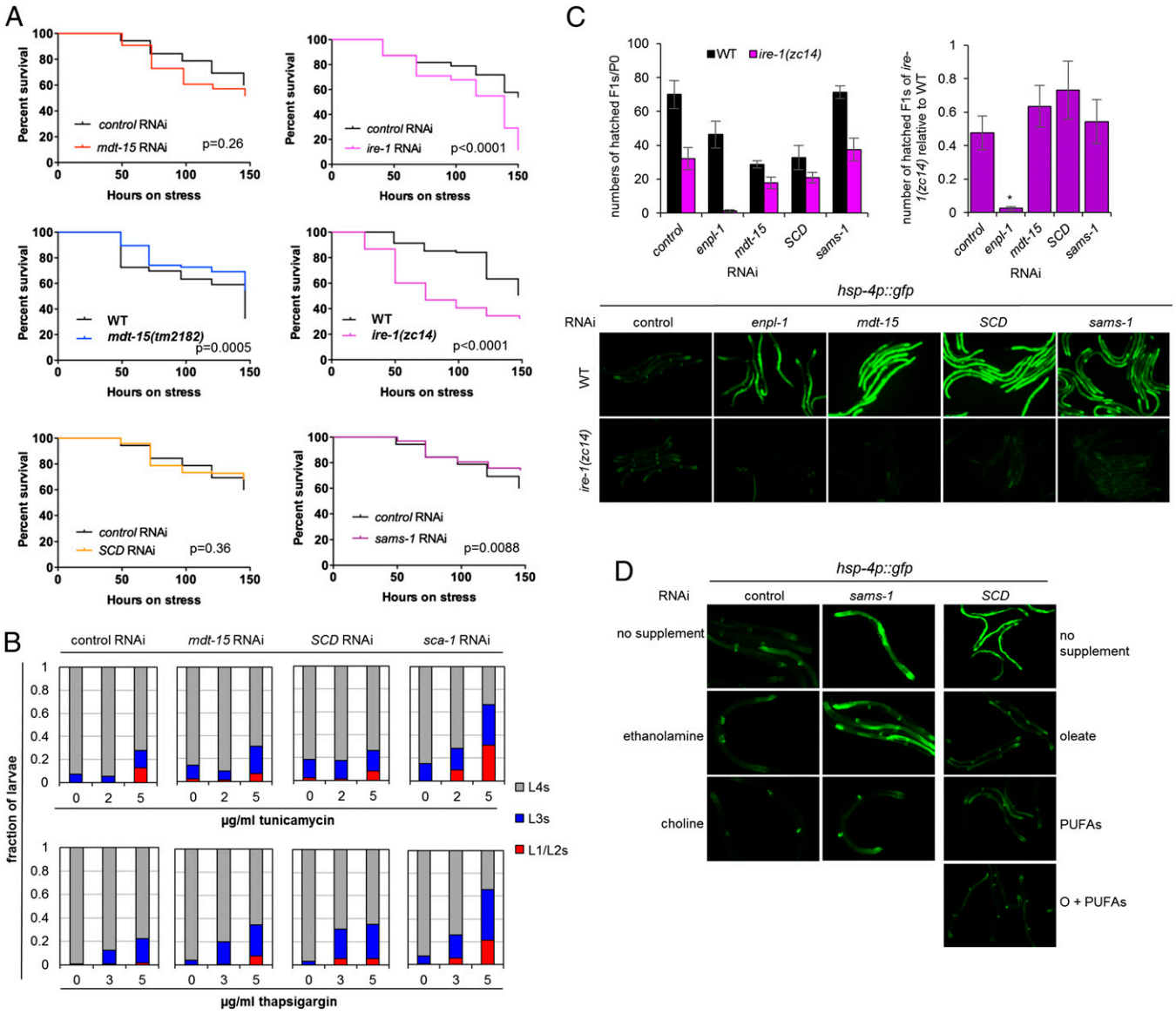

Fig. 6. *mdt-15* inactivation and defects in PL biosynthesis activate the UPR^{ER} without compromising ER protein quality control. (*A*) The plots show the survival of adult *control(RNAi)*, *mdt-15(RNAi)*, *ire-1(RNAi)*, WT, *mdt-15(tm2182)*, *ire-1(zc14)*, *SCD(RNAi)*, and *sams-1(RNAi)* worms on 30 µg/mL tunicamycin. The *P* values for *mdt-15(tm2182)* and *sams-1(RNAi)* worms indicate resistance. One of at least three independent experiments is shown; for additional replicates, see Fig. S4*A*. (*B*) Bar graphs represent the fractions of L1/L2, L3, or L4 stage *control(RNAi)*, *mdt-15(RNAi)*, and *SCD(RNAi)* larvae that are alive after 48 h on 0, 2, or 5 µg/mL tunicamycin (*Upper*) or on 0, 3, or 5 µg/mL thapsigargin (*Lower*). One of three independent experiments is shown. (*C*, *Left*) The average number of hatched F1 progeny per individual P0 WT or *ire-1(zc14)* worm grown on control, *enpl-1, mdt-15*, *SCD*, or *sams-1* RNAi. (*Right*) The ratio of hatched progeny from *ire-1(zc14)* mutants over WT worms for each RNAi treatment. $n = 4$; error bars represent SEM; $^*P < 0.05$ as determined by two-tailed unpaired Student *t* test. Micrographs below the bar graphs show WT or *ire-1(zc14)* worms carrying the *hsp-4p::GFP* reporter on control, *enpl-1*, *mdt-15*, SCD, or *sams-1* RNAi. (*D*) Micrographs depict worms expressing the *hsp-4p::GFP* reporter on control or *sams-1* RNAi with or without 30 mM ethanolamine or choline supplementation (*Left* and *Center*) and on *SCD* RNAi without supplementation (no supplement), with C18:1n-9 supplementation (oleate), with C18:2 and C20:5 supplementation (PUFAs), or with C18:1n-9, C18:2, and C20:5 supplementation (O+PUFAs) (*Right*). One of three independent experiments is shown.

resulted in CPL-1^{W32A,Y35A}::YFP accumulation (Fig. 5*B*), as reported (35). Together, these data indicate that the inactivation of genes that directly (*ire-1*, *enpl-1*, *sel-1*) or indirectly (*sca-1*) facilitate protein folding leads to enhanced aggregation of misfolded protein and triggers the UPR^{ER}, whereas *mdt-15* inactivation apparently induces the UPR^{ER} without disturbed proteostasis.

To corroborate the data obtained with molecular protein-folding markers, we next studied the sensitivity of *mdt-15* worms to two known UPR^{ER} inducers: tunicamycin and thapsigargin. Tunicamycin inhibits protein glycosylation and thus protein folding, whereas thapsigargin inhibits SCA-1 and disrupts proteostasis through its effect on ER Ca^{2+} storage (36). If the UPR^{ER} activation in *mdt-15* worms were caused by the accumulation of misfolded proteins, these animals should be hypersensitive to these proteotoxic reagents. In line with published data (30), tunicamycin shortened the life span of adult WT worms, indicating that protein misfolding compromises survival (Fig. 6*A*). Adult *mdt-15(RNAi)* worms and *mdt-15(tm2182)* mutants display constitutive UPR^{ER} (Fig. 2 *B–D*), but they were not hypersensitive to tunicamycin compared with *control(RNAi)* or WT worms (Fig. 6*A* and Fig. S4*A*). To support these results gained by studying adult worms, we also examined developmental rates as an alternate readout for tunicamycin and thapsigargin sensitivity. We found that the dose-dependent developmental arrest and lethality

throughout development caused by tunicamycin was similar in *control(RNAi)* and *mdt-15(RNAi)* worms (Fig. 6*B* and Fig. S4*B*). In contrast, *sca-1* RNAi caused substantial tunicamycin hypersensitivity, as expected (Fig. 6*B*). Similarly, *mdt-15* depletion did not lead to developmental thapsigargin hypersensitivity, whereas *sca-1* RNAi did (Fig. 6*B*). Given the otherwise broad toxin sensitivity of *mdt-15* worms (5, 7), their lack of hypersensitivity to tunicamycin or thapsigargin is especially remarkable.

Defects in the UPR^{ER} also compromise survival and growth by genetically induced proteotoxic stress (29, 30, 37). If *mdt-15* were required for the UPR^{ER} and/or proteostasis, *mdt-15* worms should exhibit synthetic lethality or growth defects with UPR^{ER} mutants. To test this hypothesis, we studied the genetic interaction between *mdt-15* and the three UPR^{ER} sensors *ire-1*, *pek-1*, and *atf-6*, whose loss of function leads to misfolded-protein aggregation in the ER (32). Specifically, to identify synthetic effects, we quantified the production of viable progeny by WT worms and *ire-1(zc14)* loss-of-function mutants (26) grown on control, *mdt-15*, or *enpl-1* RNAi and of WT worms and *atf-6(ok551)* and *pek-1(ok275)* loss-of-function mutants grown on control, *mdt-15*, or *ire-1* RNAi. As published (5, 33), *mdt-15* and *enpl-1* RNAi alone reduced progeny production in the WT background (Fig. 6*C*). However, *mdt-15* depletion did not result in synthetic embryonic lethality with the *ire-1* mutation, whereas *enpl-1* depletion did (Fig. 6*C*). Similarly, *mdt-15* RNAi did not cause synthetic embryonic lethality in combination with either the *pek-1* or the *atf-6* mutation (Fig. S5*A*); *ire-1* RNAi is effective, as demonstrated by the synthetic genetic larval arrest when combined with the *pek-1* or *atf-6* mutation (Fig. S5*B*) (28). Together, these data support the notion that *mdt-15* inactivation triggers induction of the UPR^{ER} independently of compromised ER protein quality control.

Defects in Membrane PL Composition or Synthesis Activate the UPR^{ER} Without Compromising ER Protein Folding. Because *mdt-15* maintains ER homeostasis at least in part by assuring a normal FA composition in membrane PLs, we next explored whether defects in PL synthesis per se activate the UPR^{ER} without affecting ER protein folding. Directly depleting *SCDs* [the FA Δ9-desaturases that synthesize oleic acid (C18:1n-9) and represent key *mdt-15* targets] also induced the *hsp-4p::GFP* reporter (Fig. 6 *C* and *D*). Importantly, the reduced PC polyunsaturation and the *hsp-4p::GFP* up-regulation in *SCD(RNAi)* worms were suppressed completely by dietary supplementation with oleic acid or downstream PUFAs (Fig. 6*D* and Fig. S2 *D–F*; see Tables S7–S9 for *P* values). Thus, defects in synthesizing oleic acid reduce downstream PUFA production, slightly reduce PC synthesis (Fig. S2*F*), and trigger the UPR^{ER}. Furthermore, like *mdt-15* RNAi, *SCD* depletion did not enhance ER proteotoxicity as indicated by the SRP-2^{H302R}::GFP and the CPL-1^{W32A,Y35A}::YFP reporters (Fig. 5 *A* and *B* and Fig. S3 *A* and *B*). Moreover, *SCD* RNAi did not hypersensitize *C. elegans* to tunicamycin or thapsigargin (Fig. 6 *A* and *B* and Fig. S4 *A* and *B*) and did not interact genetically with *ire-1* (Fig. 6*C*). Together, these data indicate that defects in the composition of membrane lipids can activate the UPR^{ER} independently of proteostatic stress in the ER lumen.

Alterations in membrane PC/PE ratio also activate the UPR^{ER} (13, 38). To address whether inhibiting PC synthesis induces the UPR^{ER} through impaired proteostasis, we targeted PC headgroup synthesis by depleting *sams-1*, which encodes an S-adenosyl methionine synthetase that produces the universal methyl donor S-adenosyl-methionine (Fig. S4*C*); consequently, inactivation of *sams-1* results in a substantial down-regulation of PC levels (39). As observed (39), *sams-1* RNAi up-regulated the *hsp-4p::GFP* reporter (Fig. 6 *C* and *D*). Importantly, we found that this induction was fully suppressed by supplementation with dietary choline but not ethanolamine (Fig. 6*D*), suggesting that the UPR^{ER} activation in these worms is entirely and directly caused by reduced PC levels (Fig. S4*C*). As with *mdt-15* and *SCD* RNAi, *sams-1* depletion did not cause increased SRP-2^{H302R}::GFP aggregation, tunicamycin hypersensitivity, or synthetic lethality with *ire-1* (Figs. 5*A* and 6 *A–C*). Unlike *mdt-15* and *SCD* RNAi, *sams-1* RNAi slightly raised CPL-1^{W32A,Y35A} levels, albeit much less than *sel-1* RNAi or *enpl-1* RNAi (Fig. 5*B*).

Interestingly, in contrast to *mdt-15* or *SCD* RNAi, *sams-1* RNAi strongly up-regulated the UPR^{mito} marker *hsp-6::GFP* (Fig. S6 *A–C*). This induction was completely rescued by dietary choline, suggesting that reduced PC levels disturb homeostasis in the mitochondria as well as in the ER (Fig. S6*A*). Together, these observations demonstrate that membrane lipid integrity is crucial for ER homeostasis and that defects in PL biosynthesis activate the UPR^{ER} without severely compromising proteostasis.

Discussion

Recent findings have revealed regulatory relationships between lipid biology, ER homeostasis, and disease pathogenesis (12, 13, 19, 21, 22, 38). Through the study of a lipid regulator, the Mediator subunit MDT-15, we now show that membrane lipid composition can directly influence the circuit that senses ER homeostasis. Specifically, we show that defects in PL biosynthesis caused by either altered fatty acyl unsaturation or PL headgroup synthesis constitutively activate the UPR^{ER} without compromising protein folding. A recent study showed that, in cell culture and in reconstituted liposomes, mutation of the unfolded protein sensing domains of IRE-1 and PERK does not abrogate UPR^{ER} induction upon increased membrane lipid saturation (21). Our work extends these findings by providing molecular, pharmacological, and genetic evidence for in vivo states of lipid disequilibrium that are not strictly linked to disturbed ER proteostasis.

mdt-15 regulates overall FA unsaturation (3, 4). Here, we dissected this role in greater detail and found that *mdt-15* inactivation substantially reduces FA polyunsaturation in PC; other lipid species, such as the other major *C. elegans* membrane lipid PE (40), are much less severely affected. Although there is an overall increase in monounsaturated FAs, seemingly contradicting the requirement for *mdt-15* for *SCD* expression, this increase most likely reflects a substrate build-up caused by the massive down-regulation in PUFA levels. Because the change in PC polyunsaturation was especially striking, we postulated that *mdt-15* is important for the maintenance of ER homeostasis. Indeed, multiple markers commonly used to monitor ER homeostasis were up-regulated in *mdt-15(RNAi)* worms and in the *mdt-15* hypomorph mutant. This strongly induced UPR^{ER} is partially the consequence of reduced unsaturated FA synthesis, particularly PUFAs, in *mdt-15* worms: Dietary supplementation with unsaturated FAs suppressed the defects in membrane lipid unsaturation. However, both UPR^{ER} induction and physiological phenotypes are not fully suppressed by this dietary regimen despite effective FA uptake and incorporation.

Comparisons between unsupplemented and supplemented *mdt-15(RNAi)* and *SCD(RNAi)* worms provided possible explanations for the incomplete rescue of UPR^{ER} activation. First, with supplementation, the C20:3 and C20:4 PUFA contents in PC remain down-regulated in both RNAi conditions (Fig. 2*E* and Fig. S2*E*), but the UPR^{ER} is completely restored in the supplemented *SCD(RNAi)* worms; moreover, supplemented *control(RNAi)* worms also showed reduced C20:3 and C20:4 PUFAs in PC (Fig. 2*E* and Fig. S2*E*). Thus, the reduced C20:3 and C20:4 levels in PC are unlikely to activate the UPR^{ER}. Second, in *SCD(RNAi)* worms, supplementation with the downstream PUFAs C18:2 and C20:5 rather than the SCD product C18:1n-9 was sufficient to suppress the induced UPR^{ER} fully (Fig. 6*D*). Therefore, the C18:2 and C20:5 contained in PC are likely most critical for ER homeostasis. Third, in both *mdt-15(RNAi)* and *SCD(RNAi)* worms, unsaturated FA supplementation did not eliminate the up-regulation in saturated FAs, especially C18:0 (Fig. 2*E* and Fig. S2*E*). This result is expected, because dietary rescue with downstream products should not suppress upstream substrate build-up caused by enzyme depletion. Nonetheless, in supplemented *SCD(RNAi)* worms, the UPR^{ER} is

reduced to WT level, suggesting that increased C18:0 alone is not sufficient to induce the UPR^{ER} [note that the C18:0 content in PC is similar in supplemented *mdt-15(RNAi)* and supplemented *SCD(RNAi)* worms (Fig. 2*E* and Fig. S2*E*)]. Last, *mdt-15(RNAi)* worms, but not *SCD(RNAi)* worms, also display increased C16:0 in PC, likely because of *mdt-15*'s requirement for *fat-5* expression [*fat-5* catalyzes the conversion of C16:0 to C16:1 (41)]. Exogenous C16:0 induces the UPR^{ER} in various cell lines (12, 22, 42, 43) and thus might explain the residual UPR^{ER} in *mdt-15* worms. Alternatively, it is possible that the combination of FA changes remaining in supplemented *mdt-15(RNAi)* worms underlies the residual UPR^{ER} induction.

The defective unsaturated FA synthesis in *mdt-15* or *SCD* worms triggered only the UPR^{ER} but not the UPR^{mito}, indicating a specific role for polyunsaturated PC in ER homeostasis. In contrast, disruption of choline and, by extension, PC synthesis compromised the homeostasis of both the ER and the mitochondria. Based on these observations, the ER is apparently more sensitive than the mitochondria to the unsaturation of membrane lipids, perhaps because of its greater demand for membrane fluidity and its function in lipid biosynthesis.

The lack of UPR^{mito} activation in *mdt-15(RNAi)* worms prompted us to characterize the FA composition of cardiolipin, a lipid unique to the inner mitochondrial membrane (31). Although others previously have quantified overall cardiolipin levels in worms (44), we provide here the first (to our knowledge) analysis of cardiolipin FA profiles in *C. elegans*. We found that the overall levels and the FA composition of cardiolipin were not significantly different between *control(RNAi)* and *mdt-15(RNAi)* worms, which aligns with the lack of UPR^{mito} induction. Interestingly, we found that the FA composition of *C. elegans* cardiolipin is highly unusual: More than 65% of its acyl chains consist of C20:3n-6 and C20:4n-3, whereas most eukaryotic, including mammalian, cardiolipins are composed almost exclusively of 18-carbon FAs, primarily C18:2 (31). The FA composition of *C. elegans* cardiolipin also is quite distinct from that of other *C. elegans* PL species because it is deficient in Δ5-desaturated PUFAs [20:4n-6 and 20:5; compare Fig. 1 *C* and *D* with Fig. 4*C* and Fig. S6*D* (31)]. Regulated FA composition of cardiolipin is thought to be essential for proper functioning of integral membrane proteins and for the proper formation of stacked inner-membrane cristae. Our lipid analysis suggests that the different FA compositions of the mitochondrial and ER membranes underlie the distinct cellular functions of these organelles.

Numerous studies have shown that the UPR^{ER} can be triggered by ER membrane disequilibrium, such as increased membrane PL saturation, inositol depletion, altered PC/PE ratio, and the accumulation of cholesterol in the ER membrane (12, 13, 19, 21). In these studies, the changes in lipid composition apparently activate the UPR^{ER} indirectly through protein unfolding. For example, improving proteostasis with pharmacological chaperones alleviates UPR^{ER} induction in obese mice with altered liver PC/PE ratios and in yeast with severely reduced C18:1n-9 levels (13, 38). Likewise, and in contrast to the genetic interactions we identified in *mdt-15(RNAi)*, *SCD(RNAi)*, and *sams-1(RNAi)* worms, yeast mutants with extremely low PC levels exhibit synthetic lethality in combination with an *IRE1* mutation (38). Defects in membrane PL biosynthesis, either by reducing unsaturated FAs or impairing PC production, also activated the UPR^{ER} without exacerbating misfolded-protein aggregation in the ER or hypersensitizing worms to pharmacologically or genetically induced proteotoxic stress. Our investigation thus offers an alternate perspective on how lipid disequilibrium induces the UPR^{ER}, because we observe activated UPR^{ER} without evidence of severely disturbed proteostasis.

Why do the genetic alterations observed here not cause protein unfolding but activate the UPR^{ER}? After all, the activation of the UPR^{ER} in leptin-deficient *Lep^{ob}* mice or in yeast defective for PC synthesis can be rescued by chemical chaperones (19, 20), implicating misfolded proteins as the source of ER stress in these experiments. Perhaps the lipid disturbances in the worm models used in our study are less severe than those in grossly obese *Lep^{ob}* mice or in yeast strains completely or substantially devoid of PC: Even *sams-1* worms, which experience the most substantial alterations in lipid profiles of the models we studied, undergo a relatively mild change in PC/PE ratio compared with the changes observed in the yeast *cho2* or *opi3* mutants (38). These observations may imply a threshold effect, whereby comparably mild alterations of lipid profiles activate the UPR^{ER} but do not cause the accumulation of misfolded proteins, whereas drastic changes in lipid distribution or saturation induce the UPR^{ER} through impaired proteostasis.

Unlike states of proteostatic imbalance or states of severe lipid disequilibrium, which display synthetic genetic interactions with mutations in the UPR^{ER} pathway (28–30, 37, 38), *mdt-15*, *SCD*, or *sams-1* depletion does not interact synthetically with mutations in any of the three UPR^{ER} sensors. This finding agrees with the notion that the ER stress observed in these worms is distinct from proteostatic stress. Nevertheless, it is curious that, although the UPR^{ER} is activated in *mdt-15*, *SCD*, or *sams-1* worms, its key effectors are not essential under these particular stress conditions. Perhaps other pathways act in parallel to the UPR^{ER} in these genetic contexts. Alternatively, it is possible that UPR^{ER} components play essential roles in *mdt-15*, *SCD*, or *sams-1* worms in processes not studied here, such as larval development or adult population survival.

In line with published data (13), we observed that depletion of the sarco-endoplasmic reticulum Ca^{2+}-transport ATPase SCA-1 caused severely disturbed proteostasis. Altered Ca^{2+} levels have been proposed as a link between membrane lipid saturation and UPR^{ER} activation (45) and as such represented a possible mechanism leading to the elevated UPR^{ER} in *mdt-15*–, *SCD*-, or *sams-1*–depleted worms. However, *sca-1* depletion caused substantial proteostasis defects as visualized with the neuroserpin and cathepsin reporters, and resulted in strong tunicamycin and thapsigargin sensitivity, thus presenting a phenotypic spectrum different from that found in worms with altered lipid compositions. This result suggests that the mechanism by which membrane lipid aberrancy activates the UPR^{ER} is distinct from that in *sca-1(RNAi)* worms and is largely independent of protein misfolding. Our pharmacological assays using thapsigargin did show a very slight synthetic effect with *mdt-15* or *SCD* RNAi on postembryonic development (Fig. 6*B*; see highest thapsigargin concentration). However, Ca^{2+} is essential for organism growth and survival (36, 46), as are *mdt-15* and *SCD*; thus, synthetic developmental defects are expected when Ca^{2+} homeostasis and lipid equilibrium are disturbed in combination.

In principle, the phenotypes observed in *mdt-15* worms could reflect a constitutively active UPR^{ER}, which might counteract protein misfolding. We consider this notion unlikely because our gene-expression profiling showed that, although the overlap is significant, a large fraction of UPR^{ER} genes are not induced in *mdt-15(RNAi)* worms, suggesting that these worms do not undergo a complete UPR^{ER}. Noninduced genes include many encoding ERAD machinery components (23), whose induction could have explained the lack of protein aggregates in *mdt-15(RNAi)* worms. However, *mdt-15(RNAi)*, *mdt-15(tm2182)*, *SCD(RNAi)*, and *sams-1(RNAi)* worms are not tunicamycin resistant, even at relatively low concentrations (Fig. 6*B*), and the levels of the aggregation-prone neuroserpin and of the ERAD-substrate cathepsin were not reduced (Fig. 5 *A* and *B* and Fig. S3). Hence, these worms are not protected from protein-misfolding stress as would be expected if the UPR^{ER} and/or the ERAD were activated. Possibly, the UPR^{ER} employs different upstream sensing mechanisms and generates different downstream outputs, depending on the molecular nature of the insult.

The elevated UPR^{ER} in *mdt-15* worms might be a part of a general stress response akin to the activation of cytoprotective pathways by the depletion of essential genes in *C. elegans* (34). However, this does not appear to be the case. For one, *mdt-15* inactivation does not up-regulate the UPR^{mito}, which is induced

by the inactivation of many essential genes (34). Moreover, *hsp-4* induction is not a general response to the inactivation of any essential gene; rather, it indicates the loss of an activity critical for ER function, such as protein trafficking, PL synthesis, or calcium homeostasis. Thus, induction of the UPR^{ER} implies disturbed ER function; therefore, by extension, induction of the UPR^{ER} in *mdt-15* worms reflects ER disequilibrium, not general sickness.

sams-1 inactivation activates the UPR^{ER} and the UPR^{mito} [Fig. 6*D* and Fig. S6*A* (34)], and others previously found that *sams-1* worms are long lived (47). This longevity is an interesting contrast to long-lived *daf-2*/insulin receptor mutants, in which the UPR^{ER} apparently is set at a lower threshold (48). Together, these observations suggest that the UPR^{ER} can be set at high or at low levels, and both situations can accompany longevity. It will be interesting to dissect further the relationship between the UPR^{ER} and life-span regulation and the relationship among lipid metabolism, stress responses, and longevity in general (49).

To date, MDT-15 and its orthologs have been described exclusively as coactivators, but it is formally possible that MDT-15 might serve as a corepressor at some UPR^{ER} genes; this function would explain why *hsp-4* and *xbp-1s* are induced in *mdt-15* worms. However, this supposition seems unlikely, because unsaturated FAs and *ire-1* mutation suppress *hsp-4* induction in *mdt-15* worms, demonstrating (*i*) that the observed inductions result from altered lipid profiles, and (*ii*) that *mdt-15* acts upstream of *ire-1*. Moreover, we observed an increase only of spliced, not total, *xbp-1* in *mdt-15(RNAi)* worms (Fig. 2*A*), indicating increased *ire-1*–dependent *xbp-1* processing but not elevated *xbp-1* transcription. Similar arguments hold for SAMS-1, which in principle, by virtue of synthesizing the universal methyl-group donor S-adenosyl methionine, could act through histone methylation. However, our data suggest that the UPR^{ER} in *sams-1(RNAi)* worms is induced by compromised PC synthesis, because the phenotypes caused by *sams-1* depletion can be rescued by dietary choline supplementation.

Finally, because unsaturated FA supplementation suppresses the induction of the UPR^{ER} only partially in *mdt-15* worms, there must be additional unidentified pathways under *mdt-15*'s control that promote ER homeostasis. Elevation of C16:0 may be a cause for the observed UPR^{ER} induction. Alternatively, because we previously showed that *mdt-15* regulates the response to exogenous oxidative stress (7), it is possible that *mdt-15* also is required to maintain endogenous redox balance. A compromised redox environment in *mdt-15* worms could contribute to the activated UPR^{ER}, perhaps by oxidizing ER membrane lipids. Elucidating the pathways that maintain ER homeostasis downstream of *mdt-15* will unveil new clients of the UPR^{ER}.

In summary, we propose that the UPR^{ER} is an integrative regulatory mechanism that responds both to protein-misfolding stress and to lipid imbalances in the ER membrane. It will be interesting to define the relevant players and signaling pathways further and to test whether the pathway bifurcates downstream to respond selectively to each individual stress.

Materials and Methods

Worm Strains, Growth Conditions, and RNAi. We used the following worm strains: N2 wild-type (50), NL2099 *rrf-3(pk1426) II* (51), SJ 30 *ire-1(zc14) II; zcIs4 [hsp-4p::GFP] V* (26), SJ17 *xbp-1(zc12) III;zcIs4 [hsp-4p::GFP] V* (26), *mdt-15(tm2182) III* (7), *mdt-15(tm2182) III; zcIs4 [hsp-4p::GFP] V* (this study), *mdt-15(tm2182) III; zcIs13 [hsp-6p::GFP] V* (this study), SJ4005 *zcIs4[hsp-4::GFP] V* (26), SJ4100 *zcIs13 [hsp-6p::GFP] V* (52), SJ4058 *zcIs9 [hsp-60::GFP] V* (52), *atf-6(ok551) X* (29), *pek-1(ok275) X* (28), and VK1879 *vkEx1879 [nhx-2p::cpl-1^{W32A,Y35A}::YFP; myo-2p::mCherry]* (35). To construct the *vha-6p::SRP-2^{H302R}::GFP* strain, the 1.2-kb *vha-6* promoter, full-length *srp-2*, and GFP were amplified by PCR with the following primers: TH1811 vha6_P-for+Xba1 (aatctagagcatgtacctttatagg), TH1812 vha6_P-rev+Xma1 (aacccgggtaggttttagtcgccctg), TH1861 srp-2_for +Kpn1 (aaggtaccatgtccgataacgcaacgtaag), and TH1862 srp-2_rev + Kpn1 (aaggtaccagcatgaaccccaaggaac). The resulting PCR products were cloned into the expression vector pBS already containing the *unc-54* 3′ UTR. *vha-6p::SRP-2^{H302R}::GFP* then was synthesized by site-directed mutagenesis using the Quikchange Lightning kit (no.210515; Agilent Technologies) according to the manufacturer's instructions and with the primers TH 1920 SRP_2_H302R (catctcgtcagggatccgcaaagcaatcattgaagt;) and TH1921 SRP-2_H302R_antisense (acttcaatgattgctttgcggatccctgacgagatg). Transgenic worms were generated by microparticle bombardment of *unc-119(ed4)* mutants with 10 μg of linearized DNA constructs using a Biolistic PDS-1000/HE (Bio-Rad) gene gun, as described (53).

We cultured *C. elegans* strains using standard techniques (50) and *Escherichia coli* OP50 as food source, except for RNAi. Because *mdt-15 (tm2182)* and *ire-1(zc14)* mutants display developmental delay, they were allowed to grow an extra 4 h and 1 h, respectively, to achieve developmental synchronicity with WT worms.

RNAi was performed using nematode growth medium (NGM)-RNAi plates containing 25 μg/mL carbenicillin, 1 mM isopropyl β-D-1-thiogalactopyranoside, and 12.5 μg/mL tetracycline and seeded with the appropriate HT115 RNAi bacteria. The *mdt-15*, *fat-6* (=*SCD*), *sams-1*, *ire-1*, *enpl-1*, *sel-1*, *sca-1*, and *atf-6* RNAi plasmids were from the Ahringer library (54) and were sequenced before use. We refer to *fat-6* as *SCD* because *fat-6* RNAi depletes both *C. elegans* SCDs (*fat-6* and *fat-7*) due to their sequence similarity (8). For all RNAi experiments, we acquired differential interference contrast (DIC) micrographs to document phenotypes. Tunicamycin (654380; EMD Millipore), thapsigargin (BML-PE180-00055; Enzo Life Sciences), antimycin A (A8674; Sigma), and fatty acid sodium salts (C18:1n-9, S-1120; C18:2, S-1127; C20:5, S-1144; and Nu-Chek Prep) were added at the indicated concentrations.

TLC and GC-MS. For TLC and GC-MS analysis, mid-L4 larvae were harvested in M9 buffer and washed with M9 three to four times until bacteria were no longer apparent. Then, worm pellets were snap-frozen in liquid N_2 and stored at −80 °C. Lipids were extracted, separated, and quantified using TLC and GC-MS as described, with the addition of cardiolipin standards (9, 55).

RNA Isolation and Real-Time Quantitative PCR. Developmentally synchronized L4 larvae were collected as described for GC-MC analysis; RNA isolation, and purification and real-time quantitative PCR (qPCR) were performed as described (4, 5, 7). Primer sequences are listed in Table S10. For tunicamycin induction assays, synchronized early-L4 larvae were transferred onto NGM plates containing 5 or 10 μg/mL tunicamycin and were incubated for 5 h.

DIC and Fluorescence Microscopy. Worms were picked and mounted on 2% (wt/vol) agarose pads containing NaN_3 as described (7). We captured images on a CoolSnap HQ camera (Photometrics) attached to a Zeiss Axioplan 2 compound microscope and used MetaMorph Imaging Software with Autoquant 3D digital deconvolution for image acquisition.

To monitor SRP-2^{H302R}::GFP aggregates, synchronized *vha-6p::SRP-2^{H302R}::GFP*–expressing L1 larvae were fed for 48 h with the indicated RNAi or the empty RNAi feeding vector pL4440 (control). After worms were immobilized on agarose pads with NaN_3, SRP-2^{H302R} aggregates of a defined region in the intestine were counted immediately using an Axioimager (Zeiss) with 100× magnification. We also acquired images with the Texas Red filter set to identify and eliminate autofluorescence of the gut granules. Each image illustrates the first two pairs of the anterior intestinal cells of L4 larvae or day 1 adult worms. In each experiment, aggregates of at least 15 worms per condition were monitored.

Protein Extraction and Immunoblots. Whole-worm proteins were extracted by sonication in denaturing SDS buffer with or without cOmplete Protease Inhibitor Mixture (no. 4693116001; Roche). Protein concentrations were determined using the RC DC Protein Assay kit (no. 500–0121; Bio-Rad), and SDS/PAGE analysis and immunoblotting were performed as described (4) with antibodies against Ser51-Phospho-eIF2α (no. 9721; Cell Signaling Technology), pan-actin (no. 8456; Cell Signaling Technology), tubulin (DM1A, no. T9026; Sigma), GFP (to visualize CPL-$1^{W32A,Y35A}$::YFP and *hsp-4p*–driven GFP; JL-8; BD Bioscience), and anti-rabbit HRP-conjugated (no. 7074; New England Biolabs) or donkey anti-mouse IR-Dye 800 (LI-COR) secondary antibody. Detection was done using ECL (no. 32109; Pierce) or with a LI-COR Odyssey infrared imaging system. Quantification of relative signal intensity was done using ImageJ. The arbitrary number was obtained by dividing the percentage intensity of the P-eIF2α band with that of the actin band or the percentage intensity of the YFP band with that of the tubulin band.

Developmental and Adult Drug-Sensitivity Assays. For developmental tunicamycin assays, synchronized L1s were transferred onto plates containing 0, 2, or 5 μg/mL of tunicamycin and were allowed to grow for 48 h. We scored live and dead L1/L2, L3, and L4 larvae using a light microscope; at least 100 animals were scored for each genotype or condition. Developmental thapsigargin assays were performed similarly, except that thapsigargin was added directly on top of seeded bacterial lawns for maximum efficiency, as described (36). For adult tunicamycin survival assays, synchronized L1 larvae

were cultured on NGM-RNAi plates seeded with appropriate RNAi bacteria. Early L4 larvae were transferred onto NGM-RNAi or regular NGM plates containing 30 or 40 μg/mL tunicamycin. Dead worms were scored as described (7).

Statistical Analysis. For qPCR and GC-MS analysis, we performed F-tests on at least three independent biological replicates per experiment; we then performed two-tailed Student *t* tests with equal (F-test <0.05) or unequal variance (F-test >0.05) to determine *P* values. We used GraphPad Prism 5 to generate survival curves and calculated statistical significance using the log-rank (Mantel–Cox) test.

ACKNOWLEDGMENTS. We thank Drs. C. J. Loewen, D. G. Moerman, and E. Conibear for discussions; Drs. F. C. Lynn and B. D. Lemire for critical comments on the manuscript; and the S.T. laboratory for input. S.T. holds the Canada Research Chair in Transcriptional Regulatory Networks, N.S.H. holds scholarships from the University of British Columbia (UBC) and the Child and Family Research Institute (CFRI), and D.Y.C. held a CFRI summer studentship. J.L.W. receives funding from National Institutes of Health (NIH) Grant R01 DK074114; S.T. receives funding from Canadian Institutes of Health Research Grant MOP-93713, Natural Sciences and Engineering Research Council of Canada Grant RGPIN 386398-13, the Canada Foundation for Innovation, UBC, the Center for Molecular Medicine and Therapeutics, and the CFRI; and T.H. receives funding from the Deutsche Forschungsgemeinschaft (Cologne Excellence Cluster on Cellular Stress Responses in Aging-Associated Diseases Grants FOR885, SFB635, and KFO286, and Deutsch-Israelische Projektkooperation DIP8 Grant 2014376). Some strains were provided by the Caenorhabditis Genetics Center, which is funded by the NIH Office of Research Infrastructure Programs Grant P40 OD010440.

1. Conaway RC, Conaway JW (2011) Function and regulation of the Mediator complex. *Curr Opin Genet Dev* 21(2):225–230.
2. Malik S, Roeder RG (2010) The metazoan Mediator co-activator complex as an integrative hub for transcriptional regulation. *Nat Rev Genet* 11(11):761–772.
3. Yang F, et al. (2006) An ARC/Mediator subunit required for SREBP control of cholesterol and lipid homeostasis. *Nature* 442(7103):700–704.
4. Taubert S, Van Gilst MR, Hansen M, Yamamoto KR (2006) A Mediator subunit, MDT-15, integrates regulation of fatty acid metabolism by NHR-49-dependent and -independent pathways in C. elegans. *Genes Dev* 20(9):1137–1149.
5. Taubert S, Hansen M, Van Gilst MR, Cooper SB, Yamamoto KR (2008) The Mediator subunit MDT-15 confers metabolic adaptation to ingested material. *PLoS Genet* 4(2): e1000021.
6. Fire A, et al. (1998) Potent and specific genetic interference by double-stranded RNA in Caenorhabditis elegans. *Nature* 391(6669):806–811.
7. Goh GYS, et al. (2013) The conserved Mediator subunit MDT-15 is required for oxidative stress responses in C. elegans. *Aging Cell*.
8. Brock TJ, Browse J, Watts JL (2006) Genetic regulation of unsaturated fatty acid composition in C. elegans. *PLoS Genet* 2(7):e108.
9. Watts JL, Browse J (2002) Genetic dissection of polyunsaturated fatty acid synthesis in Caenorhabditis elegans. *Proc Natl Acad Sci USA* 99(9):5854–5859.
10. Hagen RM, Rodriguez-Cuenca S, Vidal-Puig A (2010) An allostatic control of membrane lipid composition by SREBP1. *FEBS Lett* 584(12):2689–2698.
11. van Meer G, Voelker DR, Feigenson GW (2008) Membrane lipids: Where they are and how they behave. *Nat Rev Mol Cell Biol* 9(2):112–124.
12. Ariyama H, Kono N, Matsuda S, Inoue T, Arai H (2010) Decrease in membrane phospholipid unsaturation induces unfolded protein response. *J Biol Chem* 285(29): 22027–22035.
13. Fu S, et al. (2011) Aberrant lipid metabolism disrupts calcium homeostasis causing liver endoplasmic reticulum stress in obesity. *Nature* 473(7348):528–531.
14. Lagace TA, Ridgway ND (2013) The role of phospholipids in the biological activity and structure of the endoplasmic reticulum. *Biochim Biophys Acta* 1833(11):2499–2510.
15. Cao SS, Kaufman RJ (2013) Targeting endoplasmic reticulum stress in metabolic disease. *Expert Opin Ther Targets* 17(4):437–448.
16. Ron D, Walter P (2007) Signal integration in the endoplasmic reticulum unfolded protein response. *Nat Rev Mol Cell Biol* 8(7):519–529.
17. Wang S, Kaufman RJ (2012) The impact of the unfolded protein response on human disease. *J Cell Biol* 197(7):857–867.
18. Gardner BM, Walter P (2011) Unfolded proteins are Ire1-activating ligands that directly induce the unfolded protein response. *Science* 333(6051):1891–1894.
19. Pineau L, et al. (2009) Lipid-induced ER stress: Synergistic effects of sterols and saturated fatty acids. *Traffic* 10(6):673–690.
20. Ozcan U, et al. (2006) Chemical chaperones reduce ER stress and restore glucose homeostasis in a mouse model of type 2 diabetes. *Science* 313(5790):1137–1140.
21. Volmer R, van der Ploeg K, Ron D (2013) Membrane lipid saturation activates endoplasmic reticulum unfolded protein response transducers through their transmembrane domains. *Proc Natl Acad Sci USA* 110(12):4628–4633.
22. Kitai Y, et al. (2013) Membrane lipid saturation activates IRE1α without inducing clustering. *Genes Cells* 18(9):798–809.
23. Pellegrino MW, Nargund AM, Haynes CM (2013) Signaling the mitochondrial unfolded protein response. *Biochim Biophys Acta* 1833(2):410–416.
24. Heifetz A, Keenan RW, Elbein AD (1979) Mechanism of action of tunicamycin on the UDP-GlcNAc:dolichyl-phosphate Glc-NAc-1-phosphate transferase. *Biochemistry* 18(11): 2186–2192.
25. Glover-Cutter KM, Lin S, Blackwell TK (2013) Integration of the unfolded protein and oxidative stress responses through SKN-1/Nrf. *PLoS Genet* 9(9):e1003701.
26. Calfon M, et al. (2002) IRE1 couples endoplasmic reticulum load to secretory capacity by processing the XBP-1 mRNA. *Nature* 415(6867):92–96.
27. Deguil J, et al. (2011) Modulation of lipid-induced ER stress by fatty acid shape. *Traffic* 12(3):349–362.
28. Shen X, et al. (2001) Complementary signaling pathways regulate the unfolded protein response and are required for C. elegans development. *Cell* 107(7):893–903.
29. Shen X, Ellis RE, Sakaki K, Kaufman RJ (2005) Genetic interactions due to constitutive and inducible gene regulation mediated by the unfolded protein response in C. elegans. *PLoS Genet* 1(3):e37.
30. Struwe WB, et al. (2009) Modeling a congenital disorder of glycosylation type I in C. elegans: a genome-wide RNAi screen for N-glycosylation-dependent loci. *Glycobiology* 19(12):1554–1562.
31. Schlame M, Rua D, Greenberg ML (2000) The biosynthesis and functional role of cardiolipin. *Prog Lipid Res* 39(3):257–288.
32. Schipanski A, et al. (2013) A novel interaction between aging and ER overload in a protein conformational dementia. *Genetics* 193(3):865–876.
33. Natarajan B, Gaur R, Hemmingsson O, Kao G, Naredi P (2013) Depletion of the ER chaperone ENPL-1 sensitizes C. elegans to the anticancer drug cisplatin. *Worm* 2(1):e24059.
34. Melo JA, Ruvkun G (2012) Inactivation of conserved C. elegans genes engages pathogen- and xenobiotic-associated defenses. *Cell* 149(2):452–466.
35. Miedel MT, et al. (2012) A pro-cathepsin L mutant is a luminal substrate for endoplasmic-reticulum-associated degradation in C. elegans. *PLoS ONE* 7(7):e40145.
36. Zwaal RR, et al. (2001) The sarco-endoplasmic reticulum Ca2+ ATPase is required for development and muscle function in Caenorhabditis elegans. *J Biol Chem* 276(47): 43557–43563.
37. Sakaki K, et al. (2012) RNA surveillance is required for endoplasmic reticulum homeostasis. *Proc Natl Acad Sci USA* 109(21):8079–8084.
38. Thibault G, et al. (2012) The membrane stress response buffers lethal effects of lipid disequilibrium by reprogramming the protein homeostasis network. *Mol Cell* 48(1):16–27.
39. Walker AK, et al. (2011) A conserved SREBP-1/phosphatidylcholine feedback circuit regulates lipogenesis in metazoans. *Cell* 147(4):840–852.
40. Satouchi K, Hirano K, Sakaguchi M, Takehara H, Matsuura F (1993) Phospholipids from the free-living nematode Caenorhabditis elegans. *Lipids* 28(9):837–840.
41. Watts JL, Browse J (2000) A palmitoyl-CoA-specific delta9 fatty acid desaturase from Caenorhabditis elegans. *Biochem Biophys Res Commun* 272(1):263–269.
42. Cnop M, et al. (2007) Selective inhibition of eukaryotic translation initiation factor 2 alpha dephosphorylation potentiates fatty acid-induced endoplasmic reticulum stress and causes pancreatic beta-cell dysfunction and apoptosis. *J Biol Chem* 282(6): 3989–3997.
43. Wei Y, Wang D, Topczewski F, Pagliassotti MJ (2006) Saturated fatty acids induce endoplasmic reticulum stress and apoptosis independently of ceramide in liver cells. *Am J Physiol Endocrinol Metab* 291(2):E275–E281.
44. Sakamoto T, et al. (2012) Deficiency of cardiolipin synthase causes abnormal mitochondrial function and morphology in germ cells of Caenorhabditis elegans. *J Biol Chem* 287(7):4590–4601.
45. Wei Y, Wang D, Gentile CL, Pagliassotti MJ (2009) Reduced endoplasmic reticulum luminal calcium links saturated fatty acid-mediated endoplasmic reticulum stress and cell death in liver cells. *Mol Cell Biochem* 331(1-2):31–40.
46. Cho JH, Bandyopadhyay J, Lee J, Park CS, Ahnn J (2000) Two isoforms of sarco/endoplasmic reticulum calcium ATPase (SERCA) are essential in Caenorhabditis elegans. *Gene* 261(2):211–219.
47. Hansen M, Hsu A-L, Dillin A, Kenyon C (2005) New genes tied to endocrine, metabolic, and dietary regulation of lifespan from a Caenorhabditis elegans genomic RNAi screen. *PLoS Genet* 1(1):119–128.
48. Henis-Korenblit S, et al. (2010) Insulin/IGF-1 signaling mutants reprogram ER stress response regulators to promote longevity. *Proc Natl Acad Sci USA* 107(21):9730–9735.
49. Hou NS, Taubert S (2012) Function and Regulation of Lipid Biology in Caenorhabditis elegans Aging. *Front Physiol* 3:143.
50. Brenner S (1974) The genetics of Caenorhabditis elegans. *Genetics* 77(1):71–94.
51. Simmer F, et al. (2002) Loss of the putative RNA-directed RNA polymerase RRF-3 makes C. elegans hypersensitive to RNAi. *Curr Biol* 12(15):1317–1319.
52. Yoneda T, et al. (2004) Compartment-specific perturbation of protein handling activates genes encoding mitochondrial chaperones. *J Cell Sci* 117(Pt 18):4055–4066.
53. Praitis V, Casey E, Collar D, Austin J (2001) Creation of low-copy integrated transgenic lines in Caenorhabditis elegans. *Genetics* 157(3):1217–1226.
54. Kamath RS, et al. (2003) Systematic functional analysis of the Caenorhabditis elegans genome using RNAi. *Nature* 421(6920):231–237.
55. Shi X, et al. (2013) Regulation of lipid droplet size and phospholipid composition by stearoyl-CoA desaturase. *J Lipid Res* 54(9):2504–2514.